J Radioanal Nucl Chem (2013) 296:1225–1230
DOI 10.1007/s10967-012-2341-6

# Measurements of activation cross-sections for the $^{101}$Ru(n,p)$^{101}$Tc reaction for neutrons with energies between 13 and 15 MeV

**Junhua Luo · Jiuning Han · Rong Liu · Li Jiang · Suhong Ge · Zhenlai Liu · Guihua Sun**

Received: 21 September 2012 / Published online: 19 December 2012


**Abstract** In this study, activation cross-sections were measured for the $^{101}$Ru(n,p)$^{101}$Tc reaction at three different neutron energies from 13.5 to 14.8 MeV. The fast neutrons were produced via the $^{3}$H(d,n)$^{4}$He reaction on K-400 neutron generator. Induced gamma activities were measured by a high-resolution gamma-ray spectrometer with high-purity germanium detector. Measurements were corrected for gamma-ray attenuations, random coincidence (pile-up), dead time and fluctuation of neutron flux. The data for $^{101}$Ru(n,p)$^{101}$Tc reaction cross-sections are reported to be 15.7 ± 2.0, 18.4 ± 2.7 and 22.0 ± 2.4 mb at 13.5 ± 0.2, 14.1 ± 0.2, and 14.8 ± 0.2 MeV incident neutron energies, respectively. Results were compared with the previous works.

**Keywords** Ruthenium · Neutrons · Activation · Cross-sections · Nuclear reaction

## Introduction

Experimental data of neutron-induced reactions in the energy range around 13.5–14.8 MeV are needed to verify the accuracy of nuclear models used in the calculation of cross-sections. A lot of experimental data on neutron induced cross-sections for fusion reactor technology applications have been reported and great efforts have been devoted to compilations and evaluations [1, 2]. We chose to study the neutron-induced reaction cross-sections of the $^{101}$Ru(n,p)$^{101}$Tc reaction mainly for three reasons. First, ruthenium is fission product from the nuclear spent fuel. The (n,x) reaction cross-sections of ruthenium isotopes are therefore important for calculations on radiation safety of nuclear spent fuel. Second, for $^{101}$Ru(n,p)$^{101}$Tc reaction of ruthenium isotopes, ruthenium of natural isotopes composition was used as target material, it is likely that some of the studied activation products may be formed not only via the main routes but also via a few other interfering reactions. In the case of $^{101}$Ru(n,p)$^{101}$Tc reaction, special care is necessary to correct for the effect via the $^{104}$Ru(n,α)$^{101}$Mo ($T_{1/2}$ = 14.61 m, $^{101}\text{Mo} \xrightarrow{\beta^-(I_1=100\%)} {}^{101}\text{Tc}$) and the $^{102}$Ru(n,d*)$^{101}$Tc ($T_{1/2}$ = 14.22 m) processes (see Fig. 1). Third, the cross-sections of $^{101}$Ru(n,p)$^{101}$Tc reaction around 14 MeV have been measured by several groups [3–6], but most of them were obtained before 2000, furthermore, there was disagreement in those data. This is caused mainly by three factors:

1. the system difference caused by different measuring methods and experimental conditions (neutron field characteristics, radiation detector, neutron monitoring method). For the cross-sections of $^{101}$Ru(n,p)$^{101}$Tc reaction, the results of Kielan et al. [4], Kasugai et al. [3], and Kasugai et al. [5] using the gamma count method are about nine times higher than the result of Paul and Clarke [6] using beta counters method.
2. the decay data deficiencies (half-life). For $^{101}$Ru(n,p)$^{101}$Tc resction, the cross-secrions have been

J. Luo (✉) · J. Han · S. Ge · Z. Liu · G. Sun
School of Physics and Electromechanical Engineering, Hexi University, Zhangye 734000, China
e-mail: luojh71@163.com

J. Luo
State Key Laboratory of Nuclear Physics and Technology, Institute of Heavy Ion Physics, Peking University, Beijing 100871, China

R. Liu · L. Jiang
Institute of Nuclear Physics and Chemistry, Chinese Academy of Engineering Physics, Mianyang 621900, China

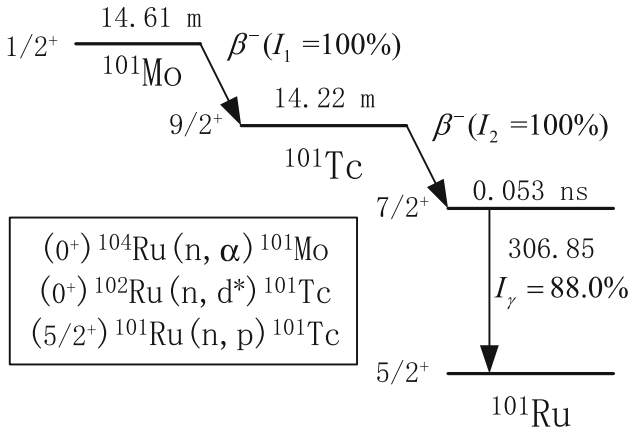


**Fig. 1** Simplified level schemes of $^{101}$Mo and $^{101}$Tc. Formation of these products via different neutron induced reactions is given together with the spin and parity of the target nuclei in parentheses [7]

determined by Paul and Clarke [6] using half-life 15.0 min. The data for 14.22 min have been measured accurately in recent years.[1]

3. interfering reactions. For $^{101}$Ru(n,p)$^{101}$Tc resction, previous work [3, 5, 6] did not consider the contribution from the $^{104}$Ru(n,α)$^{101}$Mo and $^{102}$Ru(n,d*)$^{101}$Tc reactions.

Therefore, it is necessary to make further measurements of high precision for the cross-sections of the $^{101}$Ru(n,p)$^{101}$Tc reaction.

In the present work, the cross-sections of the above mentioned reaction were measured in a neutron energy range from 13.5 to 14.8 MeV and a gamma-ray counting technique was applied using high-resolution gamma-ray spectrometer and data acquisition system. Pure ruthenium powder was used as the target material. The reaction yields were obtained by absolute measurement of the gamma activities of the product nuclei using a coaxial high-purity germanium (HPGe) detector. The neutron energies in this measurement were determined by cross-sections ratios for the $^{90}$Zr(n,2n)$^{89m+g}$Zr and $^{93}$Nb(n,2n)$^{92m}$Nb reactions [8]. The present results of $^{101}$Ru(n,p)$^{101}$Tc reaction were compared with the previous works.

## Experimental

Activation technique is very suitable for investigating low-yield reaction products and closely space low-lying isomeric states, provided their lifetimes are not too short. The details have been described over the years in many publications [9–13]. For the $^{101}$Ru(n,p)$^{101}$Tc reaction, the cross sections weren't directly measured. Rather, they were calculated relative a comparator isotope with known cross section using the detection of gamma rays from the daughter nuclei. Here we give some salient features relevant to the present measurements.

### Samples and irradiations

About 7 g of ruthenium powder of natural isotopic composition (99.99 % pure) was pressed at 10 ton/cm$^2$, and a pellet, 0.2 cm thick and 2.0 cm in diameter was obtained. Three such pellets were prepared. Monitor foils of Nb (99.99 % pure, 0.2 mm thick) and Al (99.999 % pure, 0.04 mm thick) of the same diameter as the pellets were then attached in front and at the back of each sample.

Irradiation of the samples was carried out at the K-400 Neutron Generator at Chinese Academy of Engineering Physics (CAEP) and lasted 128 min with a yield ~4–5 × 10$^{10}$ n/s. The samples position in the experiments is shown in Fig. 2. The groups of samples were placed at 0°, 90° or 135° angles relative to the beam direction and centered about the T–Ti target at distances of ~4 cm. Neutrons were produced by the T(d,n)$^4$He reaction with an effective deuteron beam energy of 134 keV and beam current of 230 μA. The tritium–titanium (T–Ti) target used in the generator was 2.18 mg/cm$^2$ thick. The neutron flux was monitored by a uranium fission chamber so that corrections could be made for small variations in the yield. Cross-sections for $^{93}$Nb(n,2n)$^{92m}$Nb or $^{27}$Al(n,α)$^{24}$Na reaction [14] were selected as monitors to measure the reaction cross-sections on $^{101}$Ru.

### Measurement of radioactivity

After having been irradiated, according to the half-life of product radioisotopes, the samples were cooled for 5–10 min, and the gamma ray activity of $^{101}$Mo, $^{101}$Tc, $^{92m}$Nb and $^{24}$Na were determined by a HPGe detector (ORTEC, model GEM 60P, Crystal diameter: 70.1 mm, Crystal length: 72.3 mm, made in USA) with a relative efficiency of ~68 % and an energy resolution of 1.69 keV at 1332 keV for $^{60}$Co. The efficiency of the detector was pre-calibrated using various standard gamma sources. The decay characteristics of the product radioisotopes and the natural abundances of the target isotopes under investigation are summarized in Table 1 [7].

### Calculation of cross-sections and their uncertainties

The measured cross-sections can be calculated by the following formula [15]:

$$\eta_x\sigma_x = \frac{[S\varepsilon I_\gamma \eta KMD]_0}{[S\varepsilon I_\gamma KMD]_x}\frac{[\lambda AFC]_x}{[\lambda AFC]_0}\sigma_0 \quad (1)$$

[1] The expression (n,d*) cross-sections used in this work includes a sum of (n,d), (n,np) and (n,pn) cross sections.

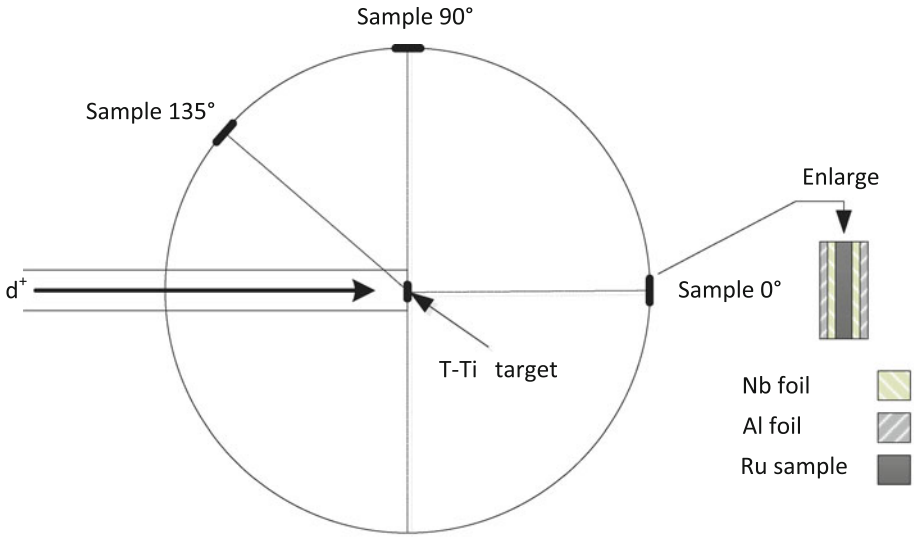


**Fig. 2** Sample position with the target assembly

**Table 1** Reactions and associated decay data of activation products

| Reaction | Abundance of target isotope (%) | $Q$-value (MeV) | Mode of decay (%) | Half-life of product | $E\gamma$ (keV) | $I\gamma$ (%) |
|---|---|---|---|---|---|---|
| $^{104}$Ru(n,α)$^{101}$Mo | 18.7 | 1.069 | $\beta^-$ (100) | 14.61 minutes | 191.92 | 19.0 |
| $^{102}$Ru(n,d*)$^{101}$Tc | 31.6 | −6.119 | $\beta^-$ (100) | 14.22 minutes | 306.85 | 88.0 |
| $^{101}$Ru(n,p)$^{101}$Tc | 17.0 | −0.83 | $\beta^-$ (100) | 14.22 minutes | 306.85 | 88.0 |
| $^{93}$Nb(n,2n)$^{92m}$Nb | 100 | −8.83 | EC (100) | 10.15 days | 934.4 | 99.07 |
| $^{27}$Al(n,α)$^{24}$Na | 100 | −3.13 | $\beta^-$ (100) | 14.959 h | 1368.6 | 100 |

where the subscript 0 represents the term corresponding to the monitor reaction and subscript $x$ corresponds to the measured reaction, $\varepsilon$ is the full-energy peak efficiency of the measured characteristic gamma-ray, $I\gamma$ is the gamma-ray intensity, $\eta$ is the abundance of the target nuclide, $M$ is the mass of sample, $D = e^{-\lambda t_1} - e^{-\lambda t_2}$ is the counting collection factor, $t_1$, $t$ is the time intervals from the end of the irradiation to the start and end of counting, respectively, $A$ is the atomic weight, $C$ is the measured full energy peak area, λ is the decay constant, $F$ is the total correction factor of the activity:

$$F = f_s \times f_c \times f_g \tag{2}$$

where $f_s$, $f_c$ and $f_g$ are correction factors for the self-absorption of the sample at a given gamma-energy, the coincidence sum effect of cascade gamma-rays in the investigated nuclide and the counting geometry, respectively. Coincidence summing correction factor $f_c$ was calculated by the method [16]. The gamma ray attenuation correction factors $f_s$ in the sample and the geometry correction $f_g$ were calculated by the following Eqs. (3) and (4), respectively.

$$f_s = \frac{\mu h}{1 - \exp(-\mu h)} \tag{3}$$

$$f_g = \frac{\left(D + h/2\right)^2}{D^2} \tag{4}$$

Here $\mu$ (in cm$^{-1}$) is the linear attenuation coefficients in ruthenium for gamma rays at each of the photon energies $E$, $h$ (in cm) is the thickness of the sample and $D$ is the distance from the measured sample to the surface of the germanium crystal.$K$ = neutron fluence fluctuation factor:

$$K = \left[\sum_i^L \Phi_i (1 - e^{-\lambda \Delta t_i}) e^{-\lambda T_i}\right] / \Phi S \tag{5}$$

Where $L$ is the number of time intervals into which the irradiation time is divided, $\Delta t_i$ is the duration of the $i$th time interval, $T_i$ is the time interval from the end of the $i$th interval to the end of irradiation, $\Phi_i$ is the neutron flux averaged over the sample during $\Delta t_i$, $S = 1 - e^{-\lambda T}$ is the growth factor of the product nuclide, $T$ = total irradiation time, $\Phi$ is the neutron flux averaged over the sample during the total irradiation time $T$

According to formula (1), we can obtain the following formula:

$$0.316\sigma(^{102}\mathrm{Ru(n,d^*)}^{101}\mathrm{Tc}) + 0.17\sigma(^{101}\mathrm{Ru(n,p)}^{101}\mathrm{Tc}) = \frac{[S\varepsilon I_\gamma \eta KMD]_0}{[S\varepsilon I_\gamma KMD]_x} \frac{[\lambda AFC]_x}{[\lambda AFC]_0} \sigma_0 \tag{6}$$

**Table 2** Summary of cross-section measurements for $^{101}$Ru(n,p)$^{101}$Tc reaction

| Reaction | References | Cross-sections (in mb) at various neutron energies (in MeV) | | |
|---|---|---|---|---|
| | | $E_n = 13.5 \pm 0.2$ | $E_n = 14.1 \pm 0.2$ | $E_n = 14.8 \pm 0.2$ |
| $^{101}$Ru(n,p)$^{101}$Tc | Present work | 15.7 ± 2.0 | 18.4 ± 2.7 | 22.0 ± 2.4 |
| $^{104}$Ru(n,α)$^{101}$Mo | [3] | 1.47 ± 0.26 | 1.92 ± 0.30 | 2.55 ± 0.33 |
| $^{102}$Ru(n,d*)$^{101}$Tc | [3] | 0.63 ± 0.07 | 1.23 ± 0.10 | 2.77 ± 0.19 |
| $^{93}$Nb(n,2n)$^{92m}$Nb | [14] | 457.9 ± 6.8 | 459.8 ± 6.8 | 459.7 ± 5.0 |
| $^{27}$Al(n,α)$^{24}$Na | [14] | 125.7 ± 0.8 | 121.6 ± 0.6 | 111.9 ± 0.5 |

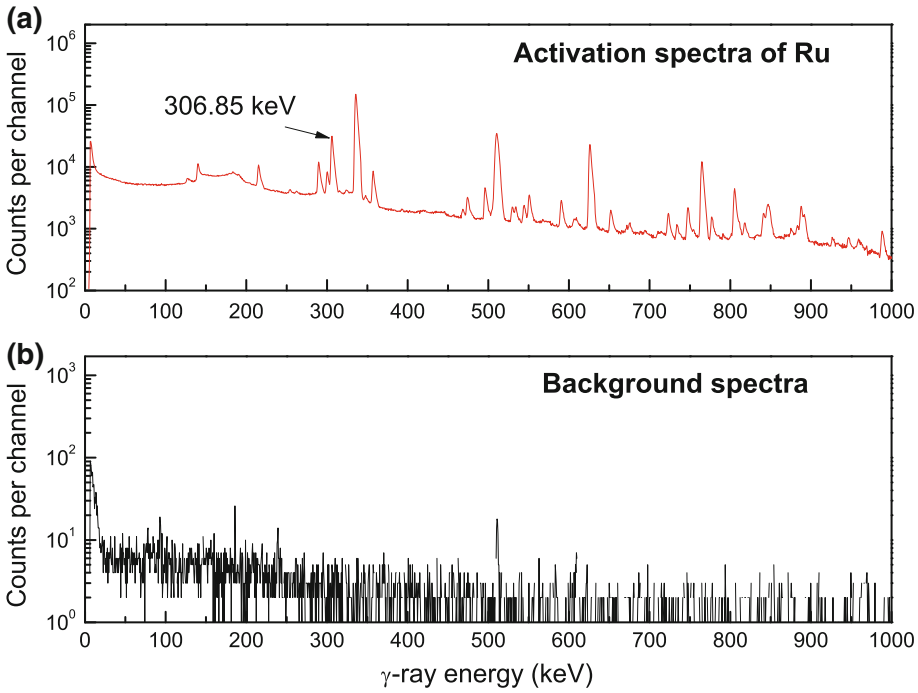


**Fig. 3** **a** The γ-ray spectra of ruthenium 480 s after the end of irradiation; **b** Background spectra

In the process of calculating the cross-sections of the $0.316\sigma(^{102}\text{Ru(n,d*)}^{101}\text{Tc}) + 0.17\sigma(^{101}\text{Ru(n,p)}^{101}\text{Tc})$ reaction, $C_x$ in (6) should be the results of actual measured full-energy peak area minus the contribution from $^{101}$Mo via $^{101}\text{Mo} \xrightarrow{\beta^-(I_1=100\%)} {}^{101}\text{Tc}$ (counting $C_1$), (see Fig. 1) [15]. According to the regulation of growth and decay of artificial radioactive nuclide, $C_1$ can be written as [17]:

$$C_1 = \frac{I_1 N_{10}\sigma_1 I_\gamma \varepsilon[S_m(\lambda_t^2 D_m - \lambda_m\lambda_t D_t) + \lambda_m(\lambda_t - \lambda_m)QD_t]}{\lambda_m\lambda_t(\lambda_t - \lambda_m)} \cdot \frac{[\lambda C]_0}{[N\sigma S D I_\gamma \varepsilon]_0} \quad (7)$$

where the subscript $m$ represents the term corresponding to the product $^{101}$Mo and $t$ corresponds to the $^{101}$Tc, $S_t = 1 - e^{-\lambda_t T}$, and $S_m = 1 - e^{-\lambda_m t_0}$; $I_1$ is branching ratio of the product $^{101}$Mo by $\beta^-$ decay, $\varepsilon$ is full-energy peak efficiency of the measured characteristic gamma-ray, $I_\gamma$ is gamma -ray intensity, $D_m = e^{-\lambda_m t_1} - e^{-\lambda_m t_2}$, $Q = [(1 - e^{-\lambda_t T}) + \frac{\lambda_t}{\lambda_t - \lambda_m}(e^{-\lambda_t T} - e^{-\lambda_m T})]$, $D_t = e^{-\lambda_t t_1} - e^{-\lambda_t t_2}$, $\sigma_1$ is cross-section of the $^{104}$Ru(n,α)$^{101}$Mo reaction, $N_{10}$ is the number of target of $^{104}$Ru(n,α)$^{101}$Mo reaction.

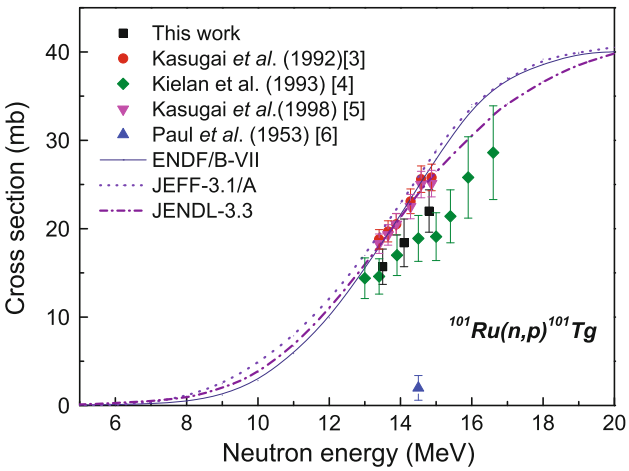


**Fig. 4** Experiment and evaluation data for $^{101}$Ru(n,p)$^{101}$Tc reaction

## Results and discussion

The advantage of the activation method with samples of the natural isotopic content lies in the fact that it produces simultaneously different reaction products, which can be easily selected because of the excellent energy resolution of the HPGe detector. It has however also the drawback that it requires a more involved analysis of the measured yields when reactions on different target isotopes lead to the same final product, e. g. there are three routes to produce $^{101}$Tc, the first via the $^{102}$Ru(n,d*)$^{101}$Tc reaction, the second via $^{101}$Ru(n,p)$^{101}$Tc reaction, and the third through the $^{104}$Ru(n,α)$^{101}$Mo reaction followed by $\beta^-$ decay. The set of differential equations (Eqs.1–7) describing formation and decay of the nuclei in question was solved to get the contributions of the investigated and the interfering reactions to the measured yield $0.316\sigma$ ($^{102}$Ru(n,d*)$^{101}$Tc) + $0.17\sigma$ ($^{101}$Ru(n,p)$^{101}$Tc). Knowing the cross-sections of the $^{104}$Ru(n,α)$^{101}$Mo reaction and of the $^{102}$Ru(n,d*)$^{101}$Tc reaction with separated isotopes from [3] are used in the present experiment.

Cross-sections values for $^{101}$Ru(n,p)$^{101}$Tc reaction on ruthenium isotopes were obtained relative to those of the $^{93}$Nb(n,2n)$^{92m}$Nb or $^{27}$Al(n,α)$^{24}$Na reaction. The main error sources in our work result from counting statistics (0.1–15 %), standard cross-sections uncertainties (1 %), detector efficiency (2–3 %), weight of samples (0.1 %), self-absorption of gamma-ray (0.5 %) and the coincidence sum effect of cascade gamma-rays (0–5 %), the uncertainties of irradiation, cooling and measuring times (0.1–1 %), etc. And some other errors contribution form the parameters of the measured nuclei and standard nuclei, such as, uncertainties of the branching ratio of the characteristic gamma rays, uncertainties of the half life of the radioactive product nuclei and so on all are considered.

The values of the $0.316\sigma$($^{102}$Ru(n,d*)$^{101}$Tc) + $0.17\sigma$ ($^{101}$Ru(n,p)$^{101}$Tc) are $2.87 \pm 0.31$, $3.52 \pm 0.42$, and $4.62 \pm 0.34$ mb at 13.5, 14.1, and 14.8 MeV incident neutron energies, respectively.

The cross-sections measured in the present work are summarized in Table 2.

One of the gamma-ray spectra is shown in Fig. 3. The 306.85 keV gamma-ray emitted in the decay of $^{101}$Tc were used to deduced the value of the $0.316\sigma$($^{102}$Ru(n,d*)$^{101}$Tc) + $0.17\sigma$($^{101}$Ru(n,p)$^{101}$Tc) reaction cross-sections. The results of this work are shown in Fig. 4 together with the literal values. From Fig. 4, we can see that our values are in agreement with Kielan et al. [4] within experimental uncertainties, but our values are lower than those obtained by Kasugai et al. [3], Kasugai et al. [5], and evaluated data of ENDF/B-VII [18], JEFF-3.1/A [19] and JENDL-3.3 [20], whereas our values are higher than data obtained by Paul and Clarke [6]. In the neutron energis of 13.5–14.8 MeV, the present data and literature data [3–5] increase with the increasing of neutron energy.

## Conclusions

We have measured the activation cross-sections for $^{101}$Ru(n,p)$^{101}$Tc reaction on ruthenium isotopes induced by 13.5, 14.1, and 14.8 MeV neutrons and a considerable improvement in accuracy was achieved. The data for $^{101}$Ru(n,p)$^{101}$Tc reaction cross sections are corrected for the calculated contributions of the $^{104}$Ru(n,α)$^{101}$Mo and the $^{102}$ Ru(n,d*)$^{101}$Tc reactions. The present results have been compared with those measured previously and with the evaluated data given in ENDF/B-VII, JEFF-3.1/A and JENDL-3.3. Our work gives more accurate measurement of cross sections for $^{101}$Ru(n,p)$^{101}$Tc reaction, during the work we used newer nuclear data for decay characteristics of the product nuclei, used a HPGe detector which has better energy resolution than Beta counter detectors that were used by early experimenters, subtracted contribution from the interfering reactions $^{104}$Ru(n,α)$^{101}$Mo and $^{102}$Ru(n,d*)$^{101}$Tc. In addition, the present measurements were performed in the Low Background Laboratory of Chinese Academy of Engineering Physics and disturbance from environmental radiation was reduced to a very low level. In conclusion, our data would improve the quality of the neutron cross-section database.

**Acknowledgments** We would like to thank the Intense Neutron Generator group at Chinese Academy of Engineering Physics for performing the irradiations. This work is supported by the National Natural Science Foundation of China (Grant No. 11165007), by the Key Project of Chinese Ministry of Education (No. 211184).

## References

1. CINDA A (2000) The index to literature and computer files on microscopic neutron data. International Atomic Energy Agency, Vienna
2. Mclane V, Dunford CL, Rose PF (1988) Neutron cross sections, vol 2. Academic, New York
3. Kasugai Y, Tokushima T, Kawade K, Yamamoto H, Katoh T, Takahashi A, Iida T (1992) Conference Report, JAERI-M Reports; No. 92,027:268
4. Kielan D, Marcinkowski A, Garuska U (1993) Isotopic effect in (n,p) reaction on ruthenium. Nucl Phys A559:333
5. Kasugai Y, Yamamoto H, Kawade K, Iida T (1998) Measurements of (n,p) cross-sections for short-lived products by 13.4–14.9 MeV neutrons. Ann Nucl Energy 25:23
6. Paul EB, Clarke RL (1953) Cross section measurements of reactions induced by neutrons of the 14.5 MeV energy. Can J Phys 31:267
7. Browne E, Firestone RB (1996) Table of isotopes. Wiley, New York

8. Lewis VE, Zieba KJ (1980) A transfer standard for d+T neutron fluence and energy. Nucl Instrum Methods 174:141
9. Luo J, Han J, Liu R, Jiang L (2012) Cross section measurements for 141Pr($n$,$\gamma$)142Pr reaction at neutron energies from 13.5 to 14.8 MeV. J Radioanal Nucl Chem 293:261
10. Rahman MM, Qaim SM (1985) Excitation functions of some neutron threshold reactions on isotopes of molybdenum. Nucl Phys A 435:43
11. Bostan M, Qaim SM (1994) Excitation functions of threshold reactions on $^{45}$Sc and $^{55}$Mn induced by 6 to 13 MeV neutrons. Phys Rev C49:266
12. Cserpák F, Sudár S, Csika J, Qaim SM (1994) Excitation functions and isomeric cross section ratios of the 63Cu(n,α)60 m, gCo, 65Cu(n,α)62 m, gCo, and 60Ni(n,p)60 m, gCo processes from 6 to 15 MeV. Phys Rev C49:1525
13. Nesaraja CD, Sudár S, Qaim SM (2003) Cross sections for the formation of 69 m, gZn and 71 m, gZn in neutron induced reactions near their thresholds: effect of reaction channel on the isomeric cross-section ratio. Phys Rev C68:024603
14. Wagner M, Vonach H, Pavlik A, Strohmaier B, Tagesen S, and Martinez-Rico J (1990) Physik Daten-Physics Data, Evaluation of Cross Sections for 14 important Neutron-dosimetry Reactions, Fachinformationszentrum Karlsruhe, Gesellschaft für wissenschaftlich-technische Information mbH, in the Federal Republic of Germany. No. 13-5
15. Luo J, Tuo F, Kong X (2011) Cross-sections for formation of $^{178m2}$Hf and $^{179m2}$Hf through reactions on natural hafnium at neutron energy 14.8 ± 0.2 MeV. J Radioanal Nucl Chem 288:143
16. McCallum GJ, Coote GE (1975) Influence of source-detector distance on relative intensity and angular correlation measurements with Ge(Li) spectrometers. Nucl Instrum Methods 130:189
17. Luo J, Tuo F, Kong X, Liu R, Jiang L (2008) Measurements of activation cross-sections for the $^{96}$Ru(n,d*)$^{95g}$Tc reaction for neutrons with energies between 13.3 and 15.0 MeV. Appl Radiat Isot 66:1920
18. Herman K, Mughabghab O (2006) ENDF/B-VII.0: Evaluated nuclear data file (ENDF), Database Version of February 2006, USA. http://www-nds.iaea.org/exfor/endf.htm
19. Forrest RA, Kopecky J, Sublet J-Ch, et al (1998) The european activation file EAF-2003 cross section library, Rep. UKAEA FUS 486
20. JENDL-3.3 (2002) Japanese evaluated nuclear data library, version-3, IAEA-NDS-110, IEAE, Vienna